Density sensitivity of intrinsic rotation profiles in ion cyclotron range of frequency-heated L-mode plasmas

PSFC/JA-12-19

Density sensitivity of intrinsic rotation profiles in ICRF-heated L-mode plasmas

M.L. Reinke, J.E. Rice, A.E. White, M. Greenwald, N.T. Howard,
P. Ennever, C. Gao, A.E. Hubbard and J.W. Hughes

July, 2012

Plasma Science and Fusion Center
Massachusetts Institute of Technology
Cambridge MA 02139 USA

This work was supported by the U.S. Department of Energy, Grant No. DE-FC02-99ER54512 and in part by an appointment to the US DOE Fusion Energy Postdocortal Research Program administered by ORISE.

Density sensitivity of intrinsic rotation profiles in ICRF-heated L-mode plasmas

M.L. Reinke, J.E. Rice, A.E. White, M. Greenwald, N.T. Howard, P. Ennever, C. Gao, A.E. Hubbard and J.W. Hughes

MIT – Plasma Science and Fusion Center, Cambridge, MA USA

ABSTRACT

The physical mechanisms that cause tokamak plasmas to rotate toroidally without external momentum input are of considerable interest to the plasma physics community. This paper documents a substantial change in both the magnitude of the core rotation frequency, $-3 < \omega(r/a=0) < +10$ kHz, and the sign of rotation shear at mid-radius, $u'=-R^2 d\omega/dr/v_{th,i,}$, which varies between $-0.6 < u' < +0.8$ in response to very small changes in the electron density. In 0.8 MA, 5.4 T Alcator C-Mod L-mode plasmas using 1.2 MW of on-axis ion-cyclotron resonance heating, plasmas with line-averaged densities from $1.0 < n_e < 1.2\times10^{20}$ m^{-3} exhibit a transition from a peaked intrinsic rotation profile to one that is hollow. Gradient scale lengths of the temperature and density profiles, the drive for plasma turbulence thought to play a role in intrinsic rotation, are indistinguishable within experimental uncertainties between the plasmas, and linear stability analysis using GYRO shows the plasmas to be in the ITG-dominated turbulence regime. The impact of changes in the rotation profile in response to minor changes in target plasma conditions is discussed in relation to established analysis techniques and cross-machine rotation scaling studies, with comparisons made to existing ASDEX-U work on intrinsic rotation shear.

I INTRODUCTION

The investigation into the phenomenon of self-generated flows in auxiliary-heated tokamak plasmas is being vigorously pursued by both the experimental [1-4] and theoretical [5-6] plasma physics community. Flow and flow shear have been shown to lead to MHD stability [7] and turbulence suppression [8], but in many tokamaks this is accomplished through applying external momentum using high power neutral beams. While toroidal rotation without momentum input has been documented on a number of experiments, the scaling of this rotation to ITER and beyond is still an open area of research [9]. If the self-generated flows are insufficient, then investment in development of torque sources for large, high density, reactor-relevant tokamaks must be made, or other external control options explored [10].

In order to have predictive capability for next-generation machines, modeling must first be shown to accurately predict flows in current devices. Alcator C-Mod [11] provides an ideal test-bed for intrinsic rotation physics as auxiliary heating, achievement of high-confinement regimes and measurement of the rotation profile are all accomplished without net momentum input. In this research, the sensitivity of the shape of the toroidal rotation profile, $\omega(r/a)$, to line-averaged electron density, n_e, is demonstrated for ICRF-heated L-mode plasmas. The rotation profile is shown to go from hollow to peaked inside of r/a ~ 0.6 as the density moves between $1.0 < n_e < 1.2\times10^{20}$ m^{-3} at B_t=5.4 T and I_p=0.8 MA. This change is likely related to the rotation reversal phenomenon previously examined in C-Mod Ohmic plasmas [12], although for those plasmas, the direction of the core rotation has been shown to change in cases where a change in sign of the rotation shear, $u'=-R^2 d\omega/dr/v_{th,i}$, at mid-radius is not observed [13]. Previous linear stability analysis in the Ohmic plasmas indicated the change in direction of the core rotation shear occurs at the transition between trapped electron mode (TEM) and ion temperature gradient (ITG) turbulence regimes occurring at the transition from Linear Ohmic Confinement (LOC) to Saturated Ohmic Confinement (SOC). Linear stability analysis using the gyrokinetic modeling code GYRO [14] shows that at r/a~0.6, the ICRF-heated C-Mod plasmas discussed here are expected to be in the ITG regime for both peaked and hollow rotation profiles.

Changes in shape of the core rotation profile have previously been observed on ASDEX-U [15] and DIII-D [16] when using electron cyclotron heating and on ASDEX-U when using ion cyclotron heating [17]. In ASDEX-U, the core rotation, expressed as Mach number, M_i, was observed to depend linearly on the off-axis rotation shear, u', with the slope of $\Delta M_i/\Delta u'$ ~ 2.0 [2] . The trend in ICRF-heated C-Mod plasmas agree well with this observation, although the relationship between core rotation and off-axis shear is smaller $\Delta M_i/\Delta u'$ ~ 0.8. This change is similar in magnitude as the ratio of major radii of the two machines, implying an increased Mach number for larger machines with similar shear in the rotation profile. The phenomenological agreement between ASDEX-U and C-Mod suggest the correlation between core M_i and off-axis shear a promising avenue for future in cross-machine rotation scaling.

Section II briefly describes the target plasmas and the diagnostic tools used in these experiments. Section III presents the results of the density scan, highlighting the changes in the magnitude of the core rotation and the shape of the profile. Section IV discusses the implications of the results for the study of intrinsic rotation and provides a brief summary.

II DESCRIPTION OF EXPERIMENT

An upper single null (USN) L-mode target plasma at I_p=0.8 MA is used, where the line-averaged density is scanned from 1.0 to 1.2×10^{20} m^{-3} from shot-to-shot, with smaller, $\Delta n_e < 10^{19}$ m^{-3}, evolution occurring during current flattop. A toroidal field of 5.4 T is used in all shots, placing the hydrogen minority resonance layer of the ICRF heating nominally on-axis, and all plasmas are heated using P_{RF}=1.2 MW of auxiliary power. The plasma features κ=1.7 and upper and lower triangularity of δ_u=0.6 and δ_l=0.3, respectively. All discharges are run with the X-point away from the direction of the ion $B\times\nabla B$ drift, i.e. unfavorable for the H-mode transition.

The electron density profile is measured using Thomson scattering, with the time-evolving, line-averaged density provided by two-color interferometry. Electron temperature profiles are also measured using Thomson scattering as well as electron cyclotron emission [18]. X-ray imaging crystal spectroscopy (XICS) [19,20] is used to determine both the ion temperature and the impurity rotation profile, using Doppler broadened and shifted line emission from H-like and He-like argon. A locked mode plasma driven by external non-axisymmetric coils is used to calibrate the wavelength scale by assuming the plasma to have ω(r/a)=0 everywhere. Soft x-ray tomography is used to provide additional estimates of the magnitude of the core-rotation by examining the sawtooth pre-cursor frequencies, which are found to agree with XICS data calibrated using the locked mode.

III RESULTS

The response of the ICRF-heated plasmas to the < 20% change in density is shown to be marginal for all kinetic properties except the toroidal rotation. Figure 1 shows the time evolution of the lowest (red) and highest (black) density plasmas used in this scan. The lower density plasma has slightly higher electron and ion temperature (b), while the stored energy as estimated from EFIT (c) is the same, as expected from the weak density scaling in L-mode. When the ICRF power (d) is applied, the line-averaged core rotation from Ar^{17+} (e) increases in the co-current direction for both, but the lower density plasma exhibits a much stronger change in rotation, increasing from – 3 kHz to +10 kHz. The higher density plasmas reaches approximately -1 kHz, an increase from the Ohmic plasma in agreement with the empirical $\Delta W/Ip$ scaling [1], shown by the dashed lines, derived from H-mode and I-mode data.

The dramatic difference in the magnitude of the core rotation is accompanied by a qualitative change in the shape of the ω(r/a) profile. Figure 2 shows the line-averaged profile of the Ar^{16+} rotation frequency for the two discharges shown in Figure 1, averaged over 0.95 < t < 1.25 seconds. Chords viewing above and below the magnetic axis are mapped to midplane minor radius, r_t, using EFIT and plotted as symbols. Outside of r/a > 0.6, the slope and magnitude of rotation profiles are the approximately the same. Just inside this radius, the higher density plasma exhibits a hollow profile while the lower density plasma maintains a strongly peaked profile. Note that in the lower density plasmas, there is no dramatic change in the slope of the ω(r/a) profile, rather the gradient outside of r/a ~ 0.6 is maintained farther into the plasma, to r/a ~ 0.4.

The electron density, temperature and ion temperature profiles averaged over this same time period are displayed in Figure 3a-c, respectively, along with their gradient scale lengths in Figures 3d-f. In 3a and 3b, 30 Thomson scattering profiles are used to compute the average profile. For each time point, a polynomial is fit to the data, and the lines in 3a and 3b are the average. In 3d and 3e, each of these 30 fits is used to calculate a gradient scale length profile, with the line representing the mean and the error bars the standard deviation. Figure 3c shows the local ion temperature profile inverted from line-averaged profiles of the Doppler broadening in H-like (solid) and He-like (dashed) Ar. While small offsets are observed between these two T_i profiles, the L_{Ti} profiles (3f) are shown to overlap within error bars. Minor changes are observed in the kinetic profiles between the two discharges, consistent with the small change in n_e, but no difference in the gradient scale length can be found outside of demonstrated uncertainty. This presents a challenge in using transport modeling to understand differences in the low and high density plasmas as discussed further in Section IV.

The target plasma was repeated multiple times with at intermediate densities of $n_e \sim 1.1\times10^{20}$ m^{-3}. These cases are displayed in Figure 4 along with the 1.0 and 1.2×10^{20} m^{-3} cases from Figure 1. The rotation is found to be inversely correlated to the density (a), with core rotation time histories (d), expressed as Mach number, $M_i=\omega R_o/v_{th,i}$, depending upon the detailed time evolution of n_e. Plasmas with density that starts low and increases a few percent over ~ 800 ms exhibit peaked rotation profiles that transition to hollow during the ICRF pulse. The change starts in the core and evolves slowly, over a few hundred milliseconds, much longer than the energy confinement time, τ_E ~ 22 ms, previously shown to be similar in magnitude to the momentum confinement time. The reverse is also true. The profile goes from hollow to peaked, when the density decreases in time. The shear in the rotation profile is normalized to the thermal velocity, $v_{th,i}$, as done in [2], and $u'=-R^2 d\omega/dr/v_{th,I}$ at r/a~0.5 (b) and r/a ~ 0.7 (c) are also documented, demonstrating that all of the shots exhibit rotation profile changes similar to those shown in Figure 2. At mid-radius, the rotation shear changes sign, going from -0.6 to nearly +0.8. Closer to the edge, u' does not display any consistent scaling with electron density at remains at approximately +2.0.

The non-linear change in the rotation shear is demonstrated in Figure 5a where u' at r/a~0.5 is plotted versus density. At $n_e=1.13\times10^{20}$ m^{-3}, the sign changes abruptly, resulting in transition from peaked to hollow rotation profiles as n_e is increased. Previous work on the core rotation reversal has shown the local collisionality, $\nu_*=0.0118 q R_o Z_{eff} n_e/(T_e^2 \epsilon^{1.5})$, to be a unifying variable [12], and the change in shape occurs between $0.10 < \nu_* < 0.15$. Figure 5b also plots the rotation shear against collisionality, including data points from USN Ohmic plasmas with the same field and current but at $0.6 < n_e < 1.2\times10^{20}$ m^{-3}. Over this density range, the direction of the core rotation changes sign, but u' ~ 0, a flat rotation profile, is observed inside of r/a~0.6 at the lowest density. In addition, the Ohmic plasmas have a smaller change in core rotation, $\Delta\omega$~7 kHz, compared to the $\Delta\omega$~12 kHz in the ICRF-heated plasmas over a smaller Δn_e. It is clear from these plasmas that local ν_* cannot be entirely responsible controlling the sign of the u' profile since the collisionality decreases monotonically with minor radius, assuming a flat Z_{eff} profile. While currently there is insufficient evidence to prove the changes in rotation shear in the ICRF-heated plasmas and the Ohmic rotation reversal are necessarily the same physics, the two share phenomenology beyond density sensitivity. In Figure 6, the line-integrated density fluctuations measured using phase-contrast imaging (PCI) [21] are shown for the shots displayed in Figure 1. For the lower density, more strongly rotating plasma, shown in 6b, there are distinct "lobes" in the dispersion spectrum that are absent in the weakly rotating plasma, shown in 6a [22]. These qualitative features have also been observed in Ohmic plasmas across rotation reversals, but require further study to decouple changes due to Doppler effect and the plasma turbulence.

IV DISCUSSION

Recent work on C-Mod and DIII-D identified correlations between core rotation and edge temperature [1] and pressure [3] gradients in enhanced confinement regimes. Although L-mode plasmas, these experiments break that link, indicating an additional mechanism that can change the rotation inside of r/a ~0.6 while maintaining a similar rotation profile at larger minor radii and a similar temperature profile. This work demonstrates two qualitatively different toroidal flow profiles at similar engineering and non-dimensional parameters, complicating attempts at cross-machine scaling of intrinsic rotation using power-law relations [9]. Future work should break the data into two groups based on the shape of the intrinsic rotation profile or produce scalings for the gradient in the rotation profile. The ($M_{i,o}$,u') data shown in Figure 4 reflects a similar relationship as shown in [2], a linear relationship with a positive slope, and represents a good starting point for the next step in intrinsic rotation scaling. The rate of change of Mach number with shear, $dM_{i,o}$/du', is weaker in Alcator C-Mod than in ASDEX-U, by a factor of ~2.5. This implies the larger machine has a larger region over which the shear is maintained, allowing the Mach number to reach a higher value in the core. Future work will extend the C-Mod database of ($M_{i,o}$,u') over Ohmic, L-mode, H-mode and I-mode plasmas.

ASDEX-U has explored the change in rotation shear in plasmas identified by GS2 linear-stability analysis to be in both the ITG and TEM turbulence regimes [2]. Although the transition from peaked to hollow did not occur at ITG/TEM transition, the most hollow rotation profiles occurred in the TEM-dominated regime. Linear stability analysis using the GYRO code was completed at r/a=0.6 for the lowest and highest density Alcator C-Mod shots discussed in this research, and at both plasmas are found to be in the ITG regime where the rotation shear changes sign. Detailed linear and non-linear GYRO simulations have been completed on C-Mod plasmas at the same I_p, B_t and n_e as the discharges discussed in this manuscript, although with 1.0 MW of ICRF power [23,24]. These results also show the plasma is ITG-dominated in the region where the rotation gradient changes. Linear simulations have found that similar target plasmas with 3.5 MW of ICRF input power exceed the linear TEM threshold, although these still exhibited a peaked rotation profile. The normalized density gradient, shown in Figure 3d, is between $2 < R/L_{ne} < 3$ for plasmas where the sign of u' changes, which is slightly higher than ASDEX-U observations in [2].

In Figure 3d-f, the gradient scale lengths for the plasmas shown in Figure 1 are documented, showing no change outside of error bars. When running non-linear gyrokinetic simulations, a common technique is to "tune" the input kinetic profiles within error bars in order to match experimental and predicted radial fluxes [25]. The observed and predicted stiffness in the turbulent-driven fluxes [26] means that small changes in scale length can lead to large changes in the cross-field energy and particle flux. Thus, similar target plasmas with matched input particle, momentum and heat fluxes that do not have statistically significant differences in the scale lengths cannot lead to differences in outputs from gyrokinetic modeling. This underscores the difficulty in using numerical simulations of isolated plasmas to understand the intrinsic rotation physics explored in this research. Rather, an approach should be to use these tools to try and match empirically observed trends, for example the threshold behavior in density or collisionality shown in Figure 5, with less emphasis on complete quantitative agreement. Future C-Mod experiments will look to cover a much wider range of ν_* by using plasmas with varying q_{95}, T_e and n_e in both ICRF-heated plasmas

The extreme sensitivity of the magnitude and shape of the rotation profile to such small changes in electron density pose a difficulty for conventional techniques used to study momentum transport in tokamaks. Perturbative transport analysis modulates a source term and studies the phase/amplitude response of a specific kinetic profile in order to understand anomalous radial transport [27]. This type of Fourier decomposition assumes a linear plasma response about some steady plasma state. If the momentum transport is investigated using modulation of the neutral beam torque, then changes in n_e or ν_*, due to the beam fueling or heating, could push the plasma through a qualitative change in the intrinsic rotation, clouding the result. Similarly if particle or thermal transport is being studied by modulating cyclotron heating, changes in ν_* due to temperature modulation could cause a change in the $\omega(r/a)$ profile and the ExB shear, possibly impacting turbulence stability. Transport experiments should include regions where the period and amplitude is increased in order to thoroughly demonstrate the linear plasma response of the target plasma. Identifying non-linear regions will not only improve the quality of the transport experiments but help to identify the cross-machine parametric dependence of these qualitative changes in the rotation profile.

In AUG [17], JET [4], DIII-D [15] others, the intrinsic rotation profile is measured using so-called “beam-blips”, in which the heating beam is turned on for a short period of time in order to make the charge exchange spectroscopy measurement. A prompt change in Doppler shift during the beam pulse is observed, and to find the background rotation profile, this $\omega(r,t)$ evolution is linearly extrapolated back to a time just prior to the use of the beam. Upgrades like those discussed in [17] are critical for having sufficient time resolution to apply this technique. Still, the beam pulses must be well spaced, at least a few momentum confinement times, in order for the unperturbed rotation profile to be restored, preventing continual, passive monitoring of the rotation profile as demonstrated here using x-ray imaging crystal spectroscopy. If near a threshold for change in the rotation profile, isolated measurements may not accurately reflect the time-averaged profiles, resulting in inconsistencies when comparing with turbulence spectra that require long-time averaging to gain statistics and knowledge of the rotation profile to understand Doppler shifts. Future work should focus on comparing CXRS and XICS measurements of intrinsic rotation in order to avoid systematic differences that could arise when combining data from the two diagnostics in cross-machine scaling.

ACKNOWLEDGEMENTS

The authors would like to thank the Alcator C-Mod team for their excellent work in maintaining and operating the tokamak, S.M. Wolfe for equilibrium reconstructions and J. Irby for interferometer measurements. We would also like to thank R. M. McDermott for useful discussions of the ASDEX-U results. This work supported by DOE contract DE-FC02-99ER54512 and in part by an appointment to the US DOE Fusion Energy Postdocortal Research Program administered by ORISE.

REFERENCES

[1] J.E. Rice, *et al*. Phys. Rev. Lett. **106** 215001 (2011)

[2] C. Angioni, *et al*. Phys. Rev. Lett. **107** 215003 (2011)

[3] W.M. Solomon, *et al*. Nucl. Fusion **51** 073010 (2011)

[4] L.-G Eriksson, *et al*. Plasma Phys. Control. Fusion **51** 044008 (2009)

[5] F.I. Parra, *et al*. Phys. Rev. Lett. **108** 095001 (2012)

[6] P.H. Diamond, *et al*. Nucl. Fusion. **47** 045002 (2009)

[7] E.J. Strait, *et al*. Phys. Rev. Lett. **74** 2483 (1995)

[8] K.H. Burrell, *et al*. Phys. Plasmas **4** 1499 (1997)

[9] J.E. Rice, *et al*. Nucl. Fusion **47** 1618 (2007)

[10] H. Zohm, *et al*. Nucl. Fusion **47** 228 (2007)

[11] E.S. Marmar, *et al*. Fusion Sci. Technol. **51** 261 (2007)

[12] J.E. Rice, *et al*. Phys. Plasmas **19** 056106 (2012)

[13] J.E. Rice, *et al.* Nucl. Fusion **51** 083005 (2011)

[14] J. Candy and R.E. Waltz, Phys. Rev. Lett. **91** 045001 (2003)

[15] R.M. McDermott, *et al*. Plasma Phys. Control. Fusion **53** 035007 (2011)

[16] J.S. deGrassie, *et al*. Phys. Plasmas **11** 4323 (2004)

[17] R.M. McDermott, *et al*. Plasma Phys. Control. Fusion **53** 124013 (2011)

[18] N. Basse, *et al*. Fusion Sci. Technol. **51** 476 (2007)

[19] A. Ince-Cushman, *et al*. Rev. Sci Instrum **79** 10E302 (2008)

[20] M.L. Reinke, *et al*. submitted to RSI (2012)

[21] M. Porkolab, *et al*. IEEE Trans. Plasma Sci. **34** 229 (2006)

[22] J.E. Rice, *et al*. Phys. Rev. Lett. **107** 265011 (2011)

[23] N.T. Howard, *et al*. Nucl. Fusion. **52** 063002 (2012)

[24] N.T. Howard, *et al*. Phys. Plasmas. **19** 056110 (2012)

[25] N.T. Howard, “Experimental and gyrokinetic studies of impurity transport in the core of Alcator C-Mod Plasmas”. PhD thesis, Massachusetts Inst. Of Tech. (2012).

[26] X. Garbet, *et al*. Plasma Phys. Control. Fusion **46** 1351 (2012)

[27] F. Ryter, *et al*. Plasma Phys. Control. Fusion **52** 124043 (2010)

FIGURE CAPTIONS

FIGURE 1: Time history of two repeated 0.8 MA, 5.4 T plasmas with ~20% difference in line-averaged electron density (a). Both are heated with 1.2 MW of ICRF power (d) and the resulting stored energy (c) and core T_e (b) are very similar, but show dramatically difference core toroidal rotation time histories (e).

FIGURE 2: Radial profile of the line-integrated toroidal rotation frequency measured from the He-like Ar Doppler shift, averaged over $0.95 < t < 1.25$ seconds.

FIGURE 3: Plots of the radial profiles of n_e (a) ,T_e (b) and T_i (c) , and their respective gradient scale length plots (d) (e) (f) for the two plasmas shown in Figure 1. The color scheme is the same as used in Figures 1 and 2.

FIGURE 4: Time history of additional repeated ICRF-heated plasmas at intermediate densities (a). Core Mach number (d) moves between the two limiting cases on long time scale. Time histories of the rotation shear, u', at r/a ~ 0.5 (b) and r/a~0.75 reveal similar shapes as shown in Figure 2.

FIGURE 5: Variation in the rotation shear, u', determined over $0.4 < r/a < 0.6$ with line-averaged density (a) and collisionality, ν_*, (b). Data from the ICRF-heated plasmas (**magenta**) are compared with a density scan in an Ohmic plasma (**blue**). Symbols for ICRF-heated shots correspond to those shown in Figure 4. For Ohmic plasmas, open circles are rotating in the counter-current direction while closed circles are the opposite.

FIGURE 6: Line-integrated density fluctuations measured using phase-contrast imaging show a qualitative change between the higher (a) and lower (b) density shots shown in Figure 1.

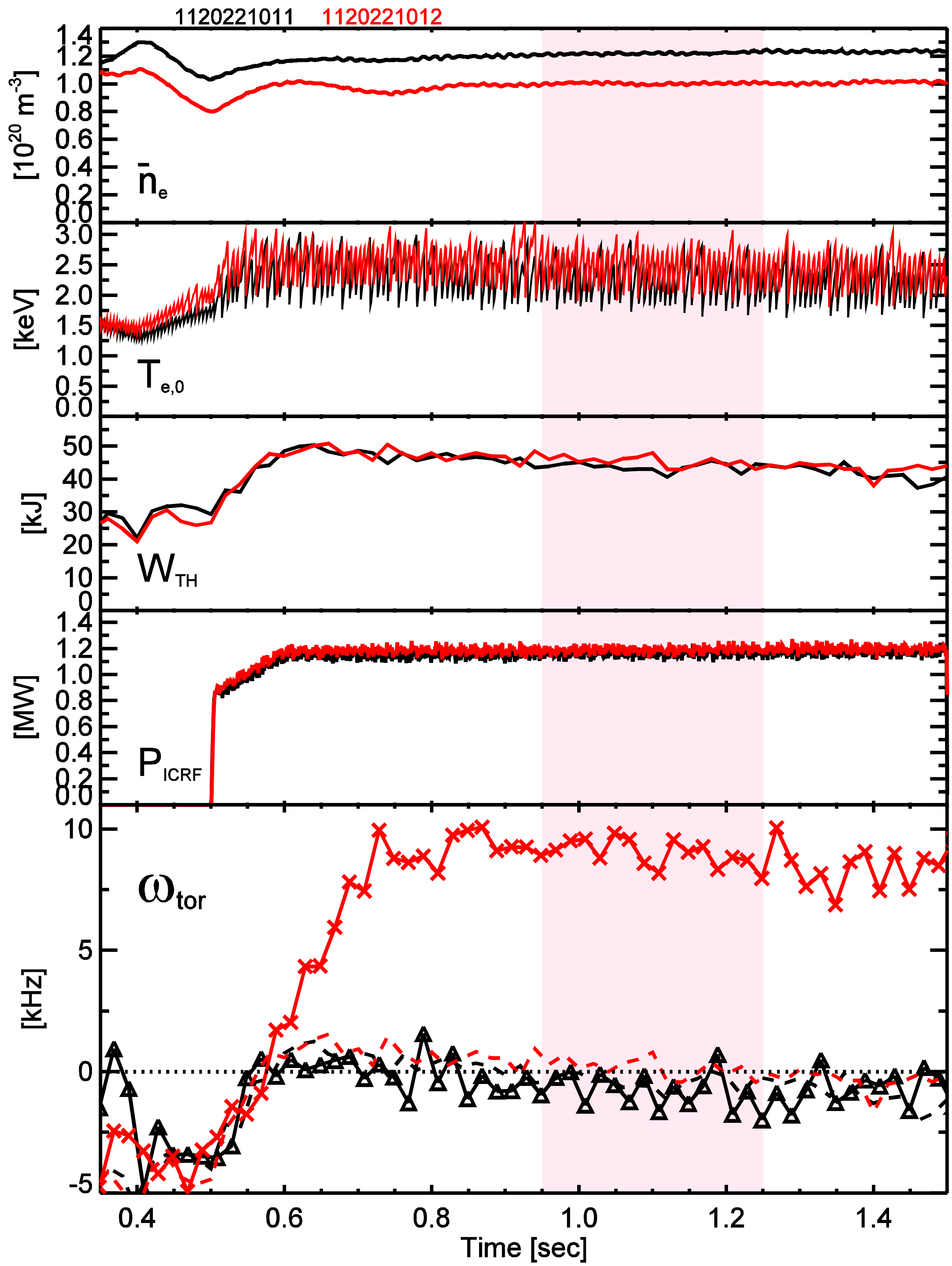
1120221011
1120221012
[10^{20} m^{-3}]
$\bar{n}_e$
[keV]
$T_{e,0}$
[kJ]
W_{TH}
[MW]
P_{ICRF}
ω_{tor}
[kHz]
Time [sec]

FIGURE 1

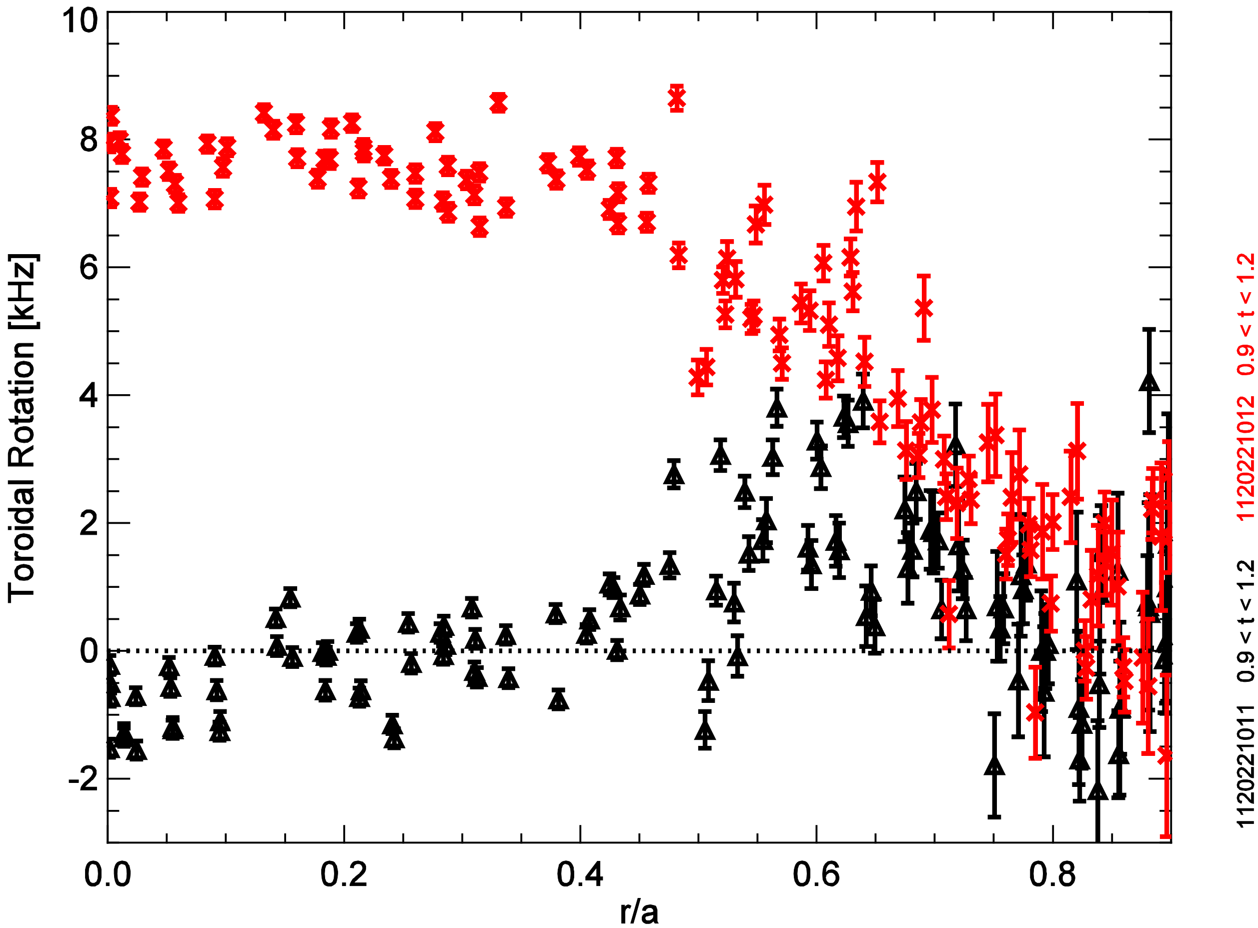
Toroidal Rotation [kHz]
r/a
1120221012 0.9 < t < 1.2
1120221011 0.9 < t < 1.2

FIGURE 2

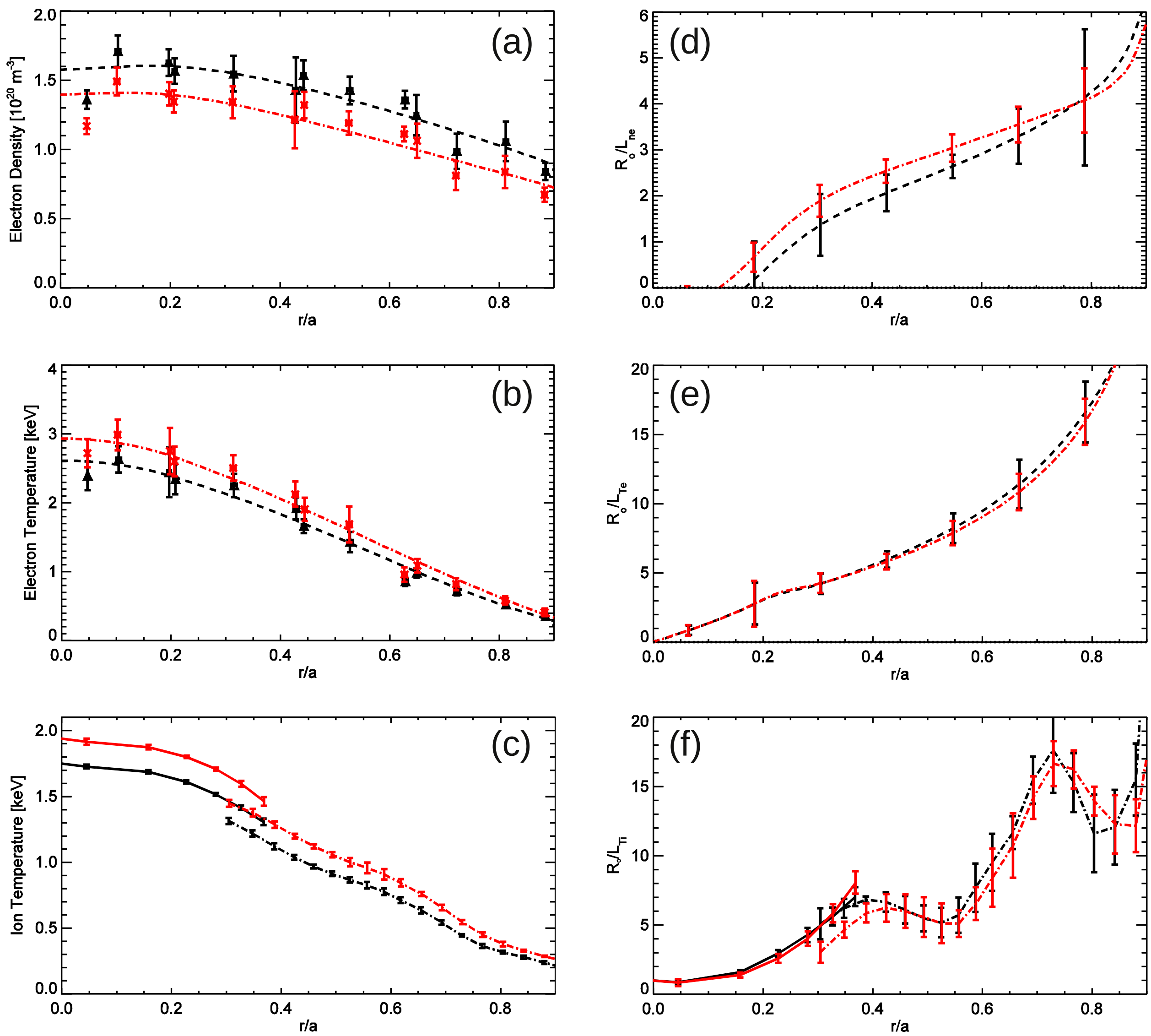
(a)
Electron Density [10^{20} m^{-3}]
r/a
(b)
Electron Temperature [keV]
r/a
(c)
Ion Temperature [keV]
r/a
(d)
R_o/L_{ne}
r/a
(e)
R_o/L_{Te}
r/a
(f)
R_o/L_{Ti}
r/a

FIGURE 3

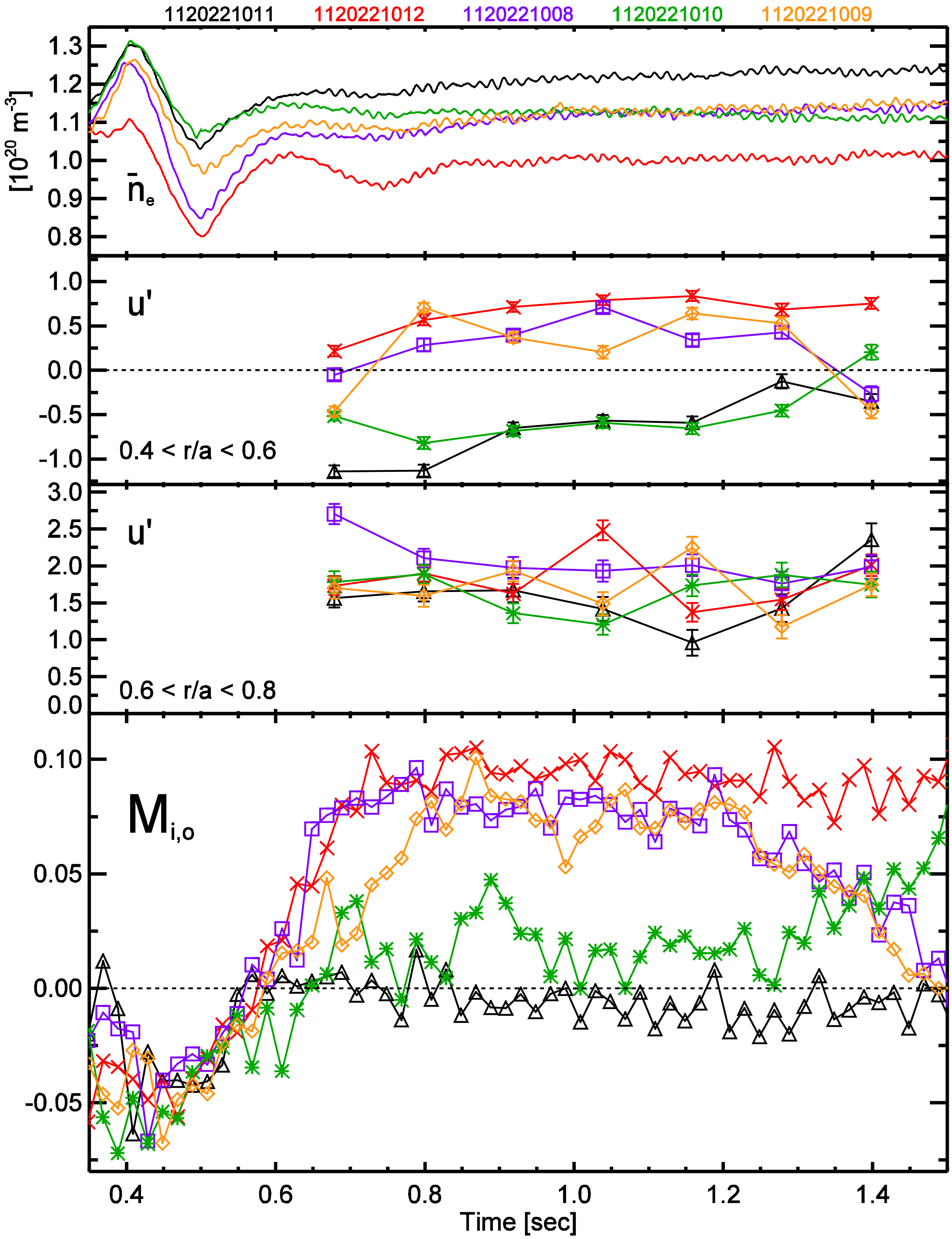

1120221011 1120221012 1120221008 1120221010 1120221009
[10^{20} m^{-3}]
$\bar{n}_e$
u'
0.4 < r/a < 0.6
u'
0.6 < r/a < 0.8
$M_{i,o}$
Time [sec]

FIGURE 4

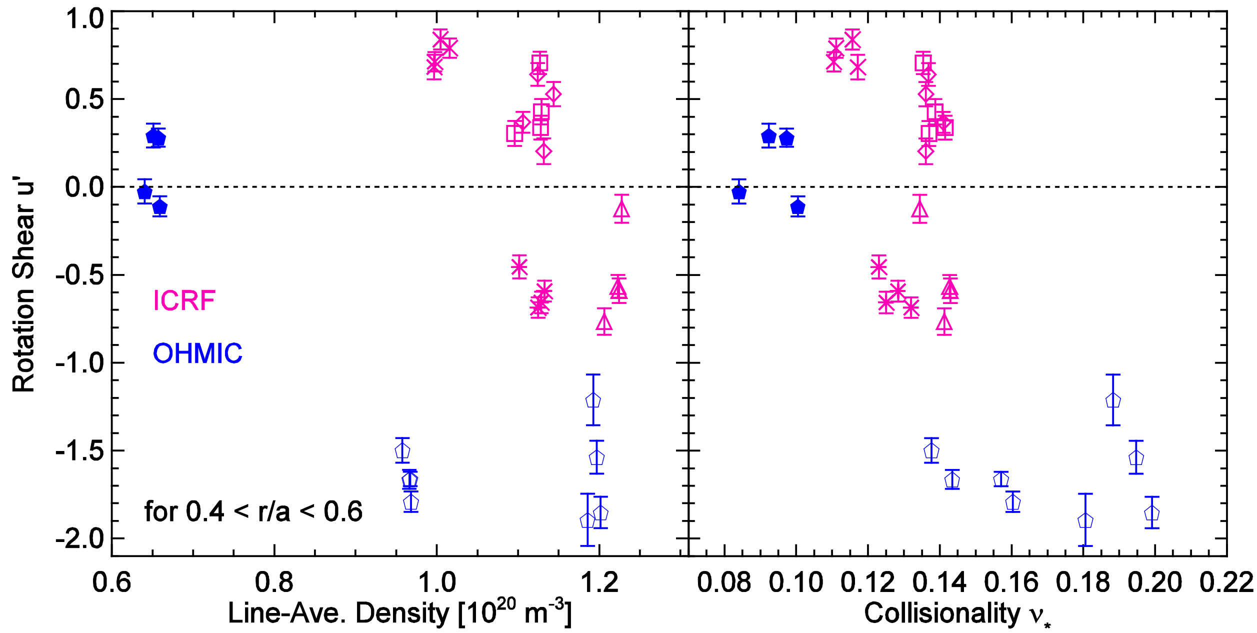

Rotation Shear u'
1.0
0.5
0.0
-0.5
-1.0
-1.5
-2.0
ICRF
OHMIC
for 0.4 < r/a < 0.6
0.6
0.8
1.0
1.2
Line-Ave. Density [10^20 m^-3]
0.08
0.10
0.12
0.14
0.16
0.18
0.20
0.22
Collisionality ν*

FIGURE 5

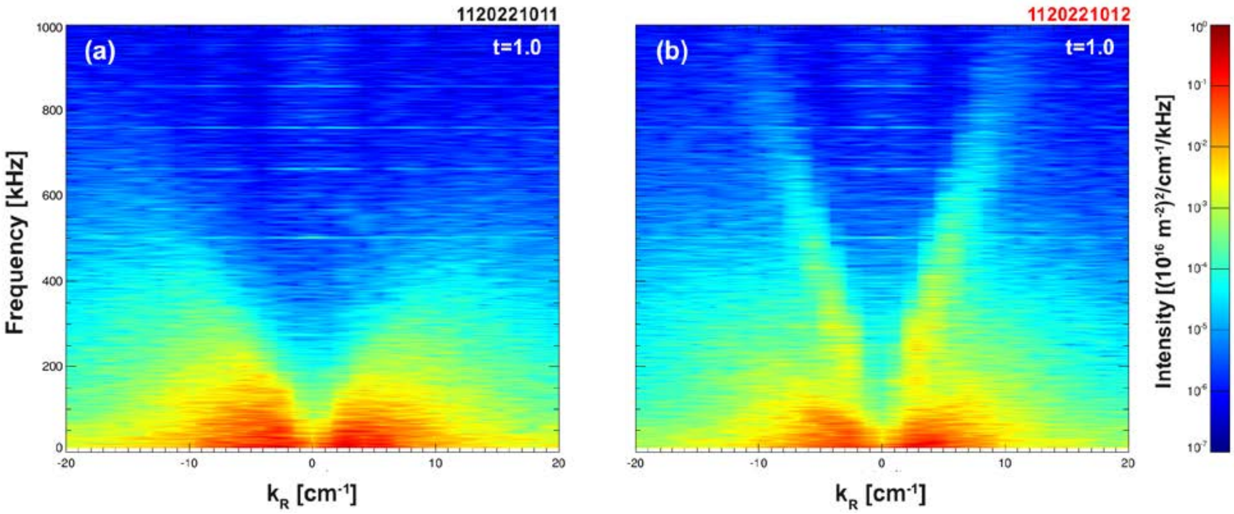
1120221011
(a)
t=1.0
Frequency [kHz]
k_R [cm^-1]
1120221012
(b)
t=1.0
k_R [cm^-1]
Intensity [(10^16 m^-2)^2/cm^-1/kHz]

FIGURE 6